ON STREAMWISE STRUCTURES IN BOUNDARY LAYER UNDER ADVERSE PRESSURE GRADIENT ON INCLINED PLATE

V. URUBA[1,2], P. PROCHÁZKA[1] AND V. SKÁLA[1]

[1] *Institute of Thermomechanics of the CAS, v. v. i.*
Dolejškova 5, Praha 8, Czech Republic

[2] *University of West Bohemia, Faculty of Mechanical Engineering*
Department of Power System Engineering, Universitní 8, Plzeň, Czech Republic

(received: 6 April 2018; revised: 7 May 2018;
accepted: 4 June 2018; published online: 12 July 2018)

Abstract: The presented study is focused on experimental investigation of a boundary layer on a flat plate in an adverse pressure gradient. The flat plate is placed in a regular flow, the pressure gradient is generated by the plate inclination. The preceding studies deal with the structure of the wake behind the plate, the presented study concentrates on the flow structure close to the suction surface of the plate. The dynamical behavior of the flow structures is studied in details with respect to the topology in the streamwise direction. In spite of the fact that the time-mean flow field is close to 2D, more or less constant along the span, the instantaneous structures topology is fully 3D. Rather oblique structures are detected instead of those oriented in the streamwise direction. The patterns are travelling in the streamwise direction along the plate.

Keywords: boundary layer, adverse pressure gradient, inclined plate, Proper Orthogonal Decomposition (POD), Oscillation Pattern Decomposition (OPD)

DOI: https://doi.org/10.17466/tq2018/22.3/f

Nomenclature

c	(m)	chord
x, y, z	(1)	dimensionless coordinates
U	(1)	dimensionless mean velocity
U_e	(m/s)	velocity of incoming flow
sum var	(1)	sum of dimensionless variances
ω	(1)	dimensionless z-component of vorticity
om var	(1)	dimensionless variance of z-component of vorticity

Abbreviations

AOA Angle of Attack
OPD Oscillation Pattern Decomposition
PIV Particle Image Velocimetry
POD Proper Orthogonal Decomposition

1. Introduction

The presented study is dedicated to experimental investigation of a boundary layer on a flat plate in an adverse pressure gradient. The flat plate is placed in a homogeneous low turbulence flow, the pressure gradient is generated by the plate inclination. Our preceding studies [1–4] were focused on the flow structure in the transversal planes, the presented paper studies the topology in the streamwise direction close to the suction surface of the plate. In this region various vortical structures emerge due to the mechanism of instability within the boundary layer subjected to an adverse pressure gradient. The presence of a streamwise vorticity component in the boundary layer is shown clearly in [1]. However, the shape of instantaneous vortices remains hidden, as the correlation of the velocity fields between the individual measuring planes perpendicular to the mean flow is unknown.

The presence of streamwise vorticity has been proved experimentally without any doubt – see *e.g.* [1–3]. The vortices are present in the suction region just above the plate, they touch the plate surface. However, the appearance of vortices in this region is random both in space (*i.e.* the position along the span) and time.

The aim of the present study is to obtain the relevant information about the topology of the vortices, especially in the streamwise direction. The streamwise vortical structures above the plate are anticipated by the "new theory of flight" proposed by Hoffman and Johnsson, see *e.g.* [5].

2. Experimental setup

A flat plate inclined with an angle of attack (AOA) of 7 degrees was placed in a uniform low turbulent stream. The blow-down facility produces a jet with a uniform velocity distribution, a mean velocity of about 5 m/s, the intensity of turbulence less than 0.2%. The plate 2 mm in thickness has rounded edges, the chord is 100 mm and the span is 450 mm. The Reynolds number based on the plate chord is about 33 000. The schematics of the experiment are shown in Figure 1.

The plane of measurement is located parallel to the plate surface at the distance from 2 up to 8 mm, defined as the constant z value. The Cartesian coordinate system is introduced with x axis in the streamwise direction parallel to the plate surface, y in the spanwise direction and z perpendicular to the plate surface. The origin of the coordinates is fixed on the upper plate surface at the centre of the leading edge (red dot in Figure 1).

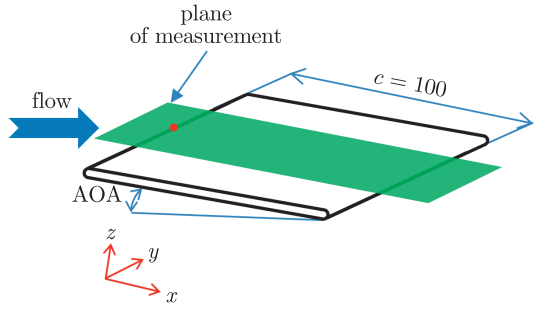

Figure 1. Schematics of the experiment

3. Methods

The experimental methods and the methods of data analysis used for the evaluation results will be described in the following section.

3.1. Instrumentation

The time-resolved PIV method was used for the experiments.

The DANTEC measuring system consisted of a double-pulse laser with cylindrical optics and a CMOS camera. For the presented experiments, the frequency was 2 kHz and 4000 double-snaps were acquired in a sequence corresponding to 2 s of the record for mean evaluation. The plane of measurement was located parallel to the plate suction surface – see Figure 1, in green. More details on the measuring technique can be found in [3].

The laser sheet thickness was approximately 1 mm, representing the uncertainty of the measurement location. If the measuring plane is well defined in a distinct distance from the surface within the boundary layer viscous sublayer, then the value of the measured velocity is proportional to the local skin friction. Our results should be considered as indicators of the flow topology close to the surface only, similar as the results of the surface flow visualization using surface paintings. The vector-lines could be supposed to follow the skin friction on the surface. However, the measurement plane location uncertainty does not allow any exact quantitative physical interpretation of the results.

3.2. Analysis methods

The acquired velocity fields series are to be subjected to further analysis. The classical statistical methods are used for determining the time mean and variances. The vorticity z-component is evaluated as well. The Proper Orthogonal Decomposition and Oscillation Pattern Decomposition methods are used to demonstrate the dynamics of the flow-field fluctuations topology.

The decomposition methods are based on the idea of a Hilbert space which is defined by snapshots forming the basis of the space. The objective of the decomposition methods is to find a different, optimized basis with a clear physical meaning.

The Proper Orthogonal Decomposition method (hereinafter POD) is looking for an orthonormal basis corresponding to modes maximizing the total variance. Each mode consists of a spatial pattern (Topos), evolution in time (Chronos) and an amplitude which is the square root of kinetic energy (or enstrophy for vorticity) of the given mode. The modes are ordered according to the decreasing amplitude.

The POD method represents a classical approach to analyze the fluctuating flow topology on the basis of the energetic content. Historically, it was introduced in the context of turbulence by Lumley [6] as an objective definition of what had been previously called big eddies and which is now widely known as coherent structures.

The Oscillation Pattern Decomposition method (hereinafter OPD) evaluates oscillating modes and is based on ideas formulated by Hasselmann [7]. The OPD method consists in the stability assessment of fluctuation patterns in the flow under study and it provides a set of the OPD modes. Each mode is characterized by its frequency, a damping factor called e-folding time and topology. The quasi-periodical behavior is supposed with the given frequency and decaying amplitude, the mean time period for its decay by factor e is given by the e-folding time. The mode topology is defined by a complex spatial mode, the real and imaginary parts characterize fluctuating flow patterns shifted by a quarter of period, respectively.

More details on the OPD method can be found *e.g.* in [7–9].

4. Results

All the presented results are given in a non-dimensional form, the coordinates are divided by the plate chord, $c = 100\,\mathrm{mm}$, the velocities – by the inlet velocity $U_e = 5\,\mathrm{m/s}$ and the variances by the square thereof. The vorticity is normalized by the factor $U_e/c = 50\,1/\mathrm{s}$. The OPD and POD modes are non-dimensional by definition, as their amplitudes are normalized by the mathematical algorithm.

The results are evaluated in measuring planes in 4 distances from the suction plate surface $z = 0.02$, 0.04, 0.06 and 0.08, however a detailed analysis will be shown for the measuring plane closest to the surface $z = 0.02$. The measuring planes farther from the surface are acquired only to check the flow evolution within the boundary layer – see Figures 2 and 3 in the next chapter.

4.1. Statistics

The time mean flow-field will be shown first. In Figures 2 and 3 the streamwise (x) mean velocity component and the sum of both the evaluated velocity component variance distributions are shown respectively in the whole inspected domain.

Figures 2 and 3 show the series of isosurfaces of relevant quantities.

In Figures 4 and 5 the same quantities are depicted within the measuring plane $z = 0.02$. The spanwise mean velocity component approaches zero in the whole domain.

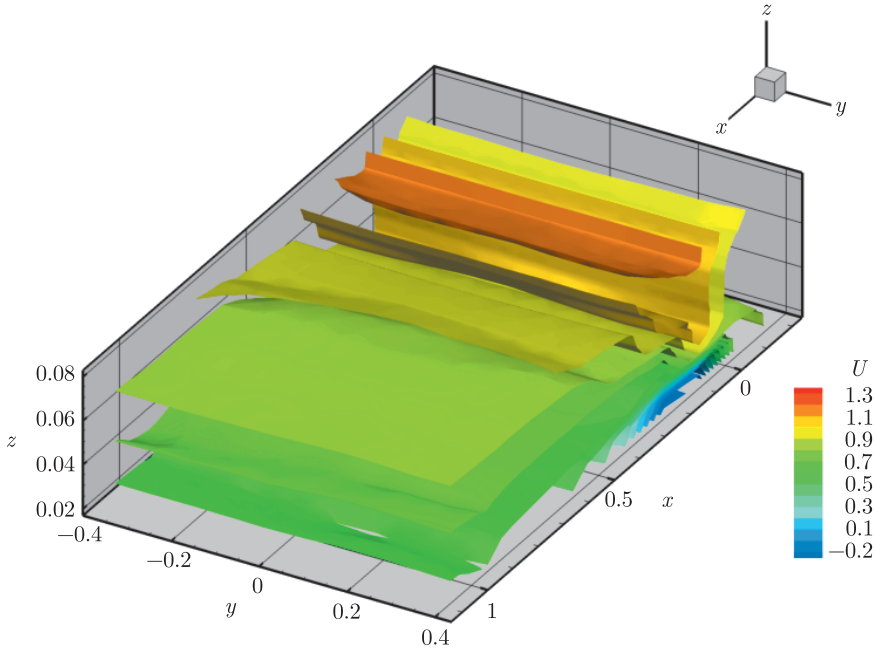

Figure 2. Iso-surfaces of mean streamwise velocity component

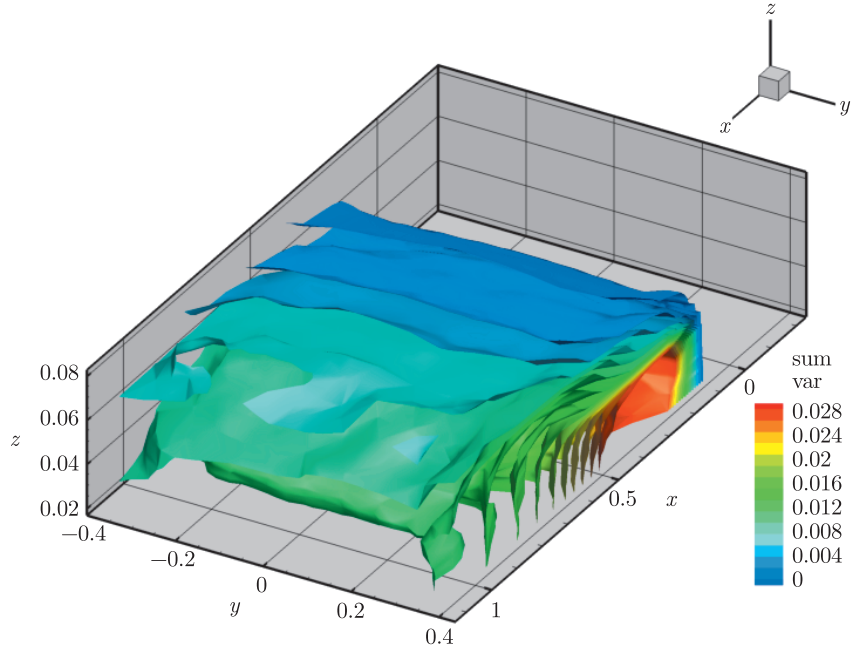

Figure 3. Iso-surfaces of the sum of velocity component variances

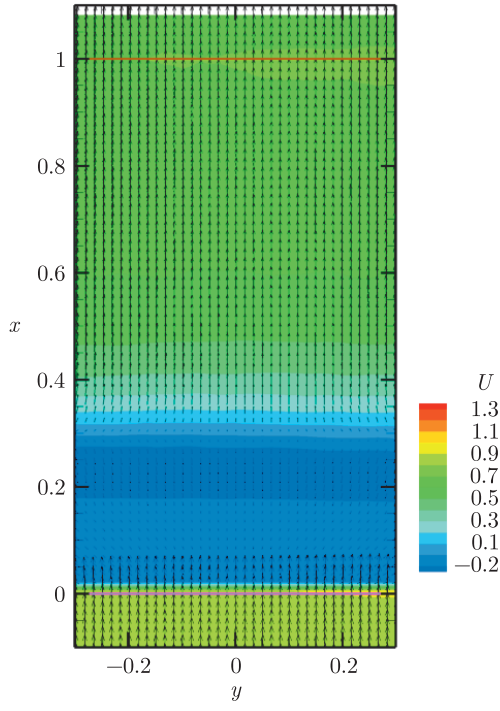

Figure 4. Mean velocity distribution

In Figures 4 and 5 the lines $x = 0$ and $x = 1$ indicate the positions of the leading and trailing edges, respectively. In Figures 2 and 4 the dark blue color indicates the negative streamwise velocity component, meaning the back-flow region caused by the flow separation on the leading edge and the reattachment close to the position $x = 0.25$. There is a region of streamwise velocity overshoot above the separation zone, the velocity exceeds the free stream value (*i.e.* it is over 1). The maximum dynamical activity region is located just downstream of the reattachment point – see the red color in Figures 3 and 5.

The results indicate clearly that the time-mean flow-field is more or less 2D, the distributions are independent on the position y across the span.

For the subsequent dynamical analysis the domain was in the streamwise direction limited to the region with the attached boundary layer $0.25 < x < 1$, *i.e.* between the reattachment point and the trailing edge.

4.2. OPD analysis of velocity fields

The OPD method was applied on the velocity vector distribution time-resolved data in the measuring plane $z = 0.02$, the 10 OPD modes were evaluated.

The Parameters of all OPD modes are given in Table1, in Figure 6 these are the modes in the frequency – periodicity plain. The 3 modes nos. 1, 5 and 8 with the largest value of periodicity were selected for presentation. These are true oscillating modes represented by traveling patterns in the streamwise direction.

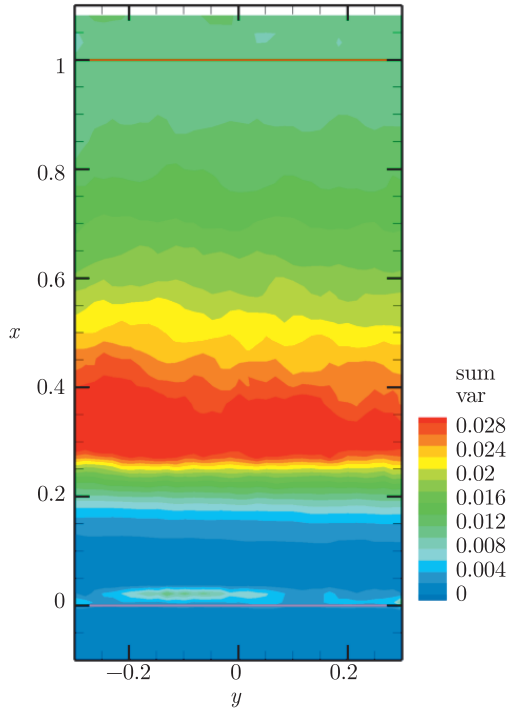

Figure 5. Sum of velocity component variance distribution

Table 1. OPD modes

mode	frequency (Hz)	e-folding time (ms)	Periodicity (1)
1	104.0	23.3	2.42
2	61.8	22.3	1.38
3	34.8	22.2	0.77
4	29.9	21.6	0.64
5	117.5	21.2	2.49
6	42.6	20.6	0.88
7	76.6	17.7	1.36
8	133.0	15.2	2.02
9	0	14.8	0
10	0	12.0	0

The modes with a low periodicity value or even 0 (modes 9 and 10) are of a pulsating or decaying nature, not moving in space.

The spatial patterns will be shown for the selected modes, in Figures 7 (a), (b) there are real and imaginary parts of OPD mode 1, respectively.

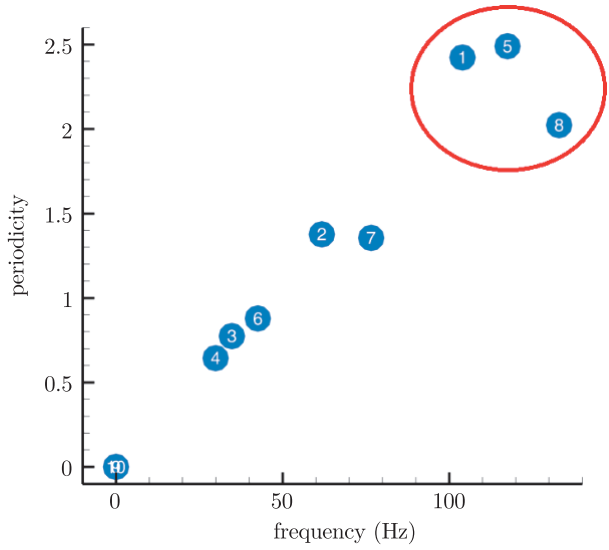

Figure 6. OPD spectrum, periodicity and frequencies of OPD modes

The mode topology is represented by a velocity vector pattern and a color field representing the vorticity component perpendicular to the surface: red positive, blue negative values – see the legend in Figure 7 (c).

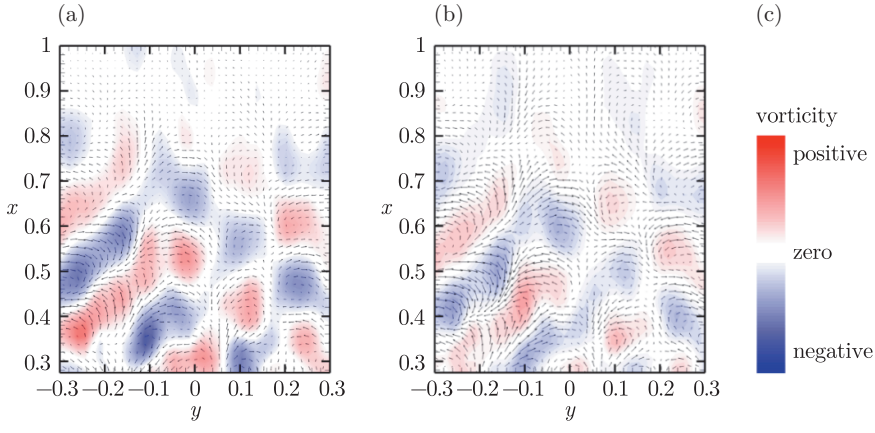

Figure 7. Real (a) and imaginary (b) parts of OPD mode 1, (c) vorticity legend

The patterns in the real and imaginary parts of OPD mode 1 are very similar, there is only a difference in the position of the patterns in the streamwise direction and intensity. The intensity difference means that the amplitude of patterns changes periodically. The shift in space is connected with movement of patterns in the streamwise direction. The spacing of the structures is about 0.03, divided by the mode period in time, it results in the pattern velocity of about 3 m/s, representing about 62% of the incoming velocity.

The OPD modes 5 and 8 are shown in Figures 8 and 9, Figure (a) represents the real part and (b) the imaginary part, respectively. The imaginary part is again shifted in x direction resulting in the streamwise velocity of the pattern.

The studied OPD modes consist of shear layers, visible as the vorticity concentration, in a zigzag configuration.

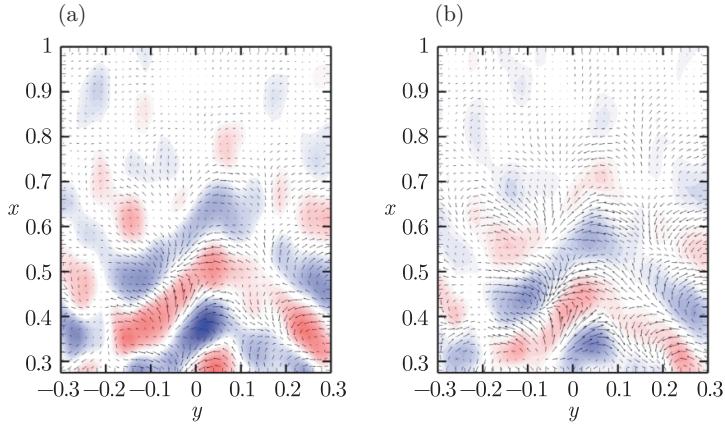

Figure 8. Real (a) and imaginary (b) parts of OPD mode 5

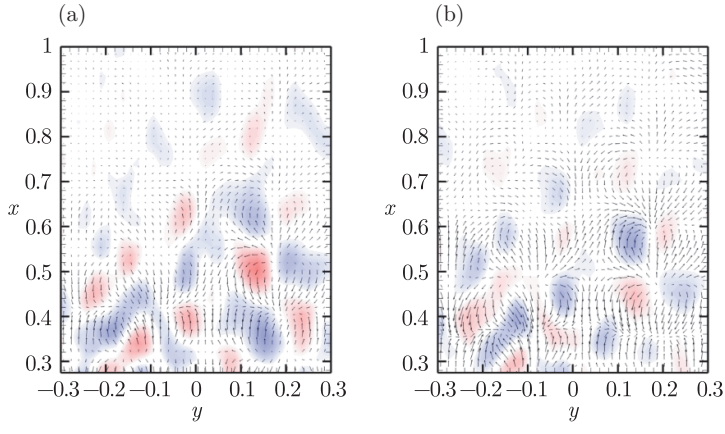

Figure 9. Real (a) and imaginary (b) parts of OPD mode 8

The OPD mode 8 topology is falling into spots, but still the zigzag pattern is visible.

4.3. POD analysis of vorticity fields

The vorticity z-component ω was evaluated from all the individual velocity vector fields. In Figure 10, there is a distribution of the vorticity variance. The mean value of vorticity is very small in magnitude, smaller by one order in comparison with instantaneous vorticity values. The maximum of the fluctuating activity is located just behind the boundary layer reattachment, the vorticity

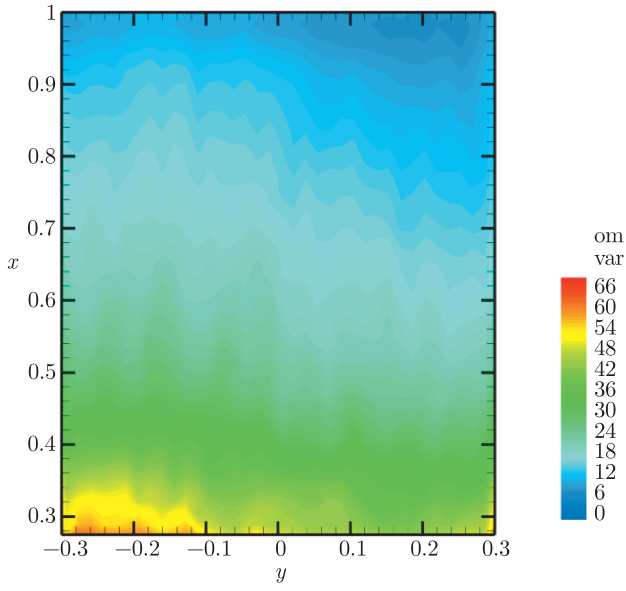

Figure 10. Vorticity variance distribution

variance distribution is close to the 2D distribution, similar as for the velocity (compare Figures 4 and 5).

The resulting vorticity fields were subjected to the POD analysis to determine the modes explaining the vorticity variance, which could be considered as an enstrophy part. Figure 11 shows the enstrophy fraction and the accumulated enstrophy of the vorticity POD modes depicted for all 2000 modes. The first POD mode contains 1.3% of the total enstrophy, while the first 10 modes cover about 11%.

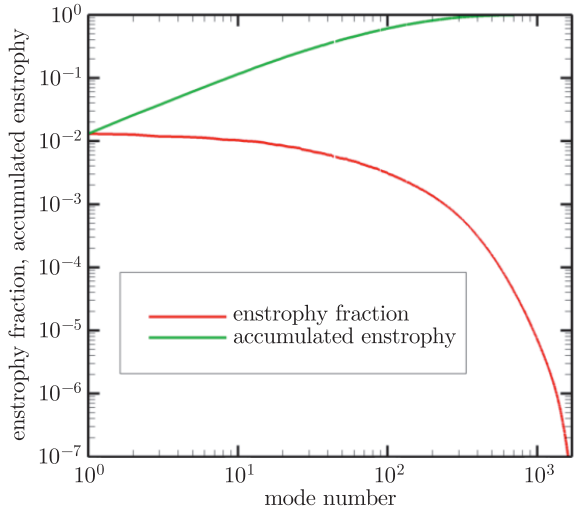

Figure 11. Enstrophy fraction and accumulated enstrophy of vorticity POD modes

The selected POD mode topologies will be shown. Figure 12 (a) shows the POD mode 1 as the vorticity fluctuations distribution – Topos. Figure 12 (b) shows the corresponding time evolution of the mode, obtained as a projection of the mode topology on the velocity vector field time series – Chronos. The vorticity legend in Figure 12 (c) shows the meaning of the colors in the Topos depiction, it has only a qualitative meaning within the given mode, as the modes are normalized.

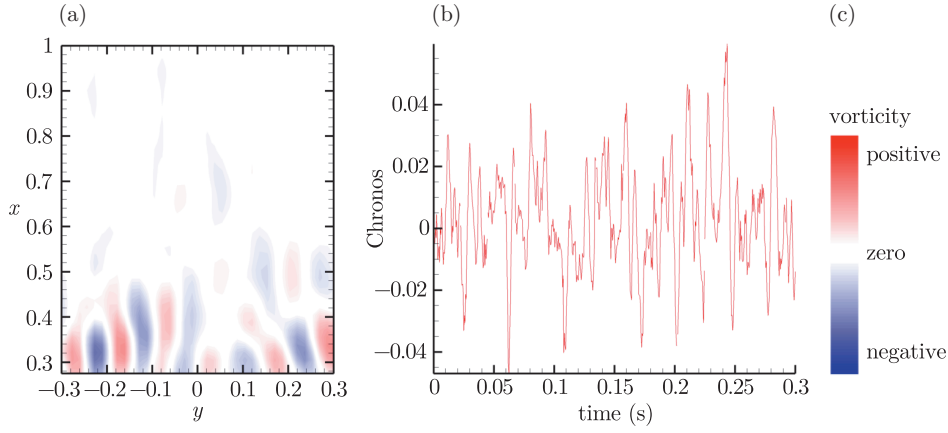

Figure 12. Topos (a) and Chronos (b) of POD mode 1, (c) vorticity legend

The examples of higher order POD modes containing lower energy are shown in the following Figures. In Figure 13 POD mode 4, in Figure 14 POD mode 40 and in Figure 15 POD mode 99 are depicted in the form of Topos (a) and Chronos (b).

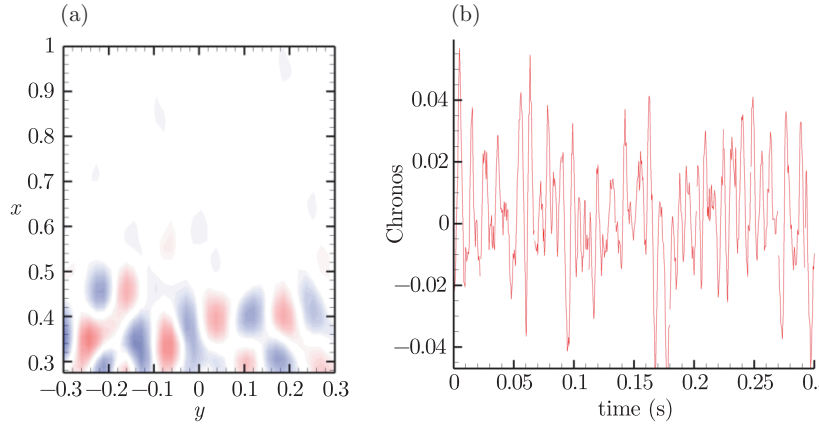

Figure 13. Topos (a) and Chronos (b) of POD mode 4

The patterns consist of vorticity strips in the streamwise and/or oblique directions, filling the region behind the point of reattachment. Higher order modes

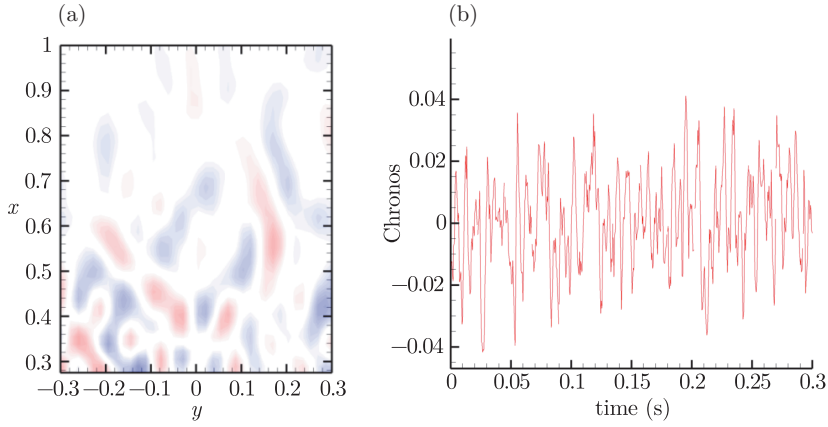

Figure 14. Topos (a) and Chronos (b) of POD mode 40

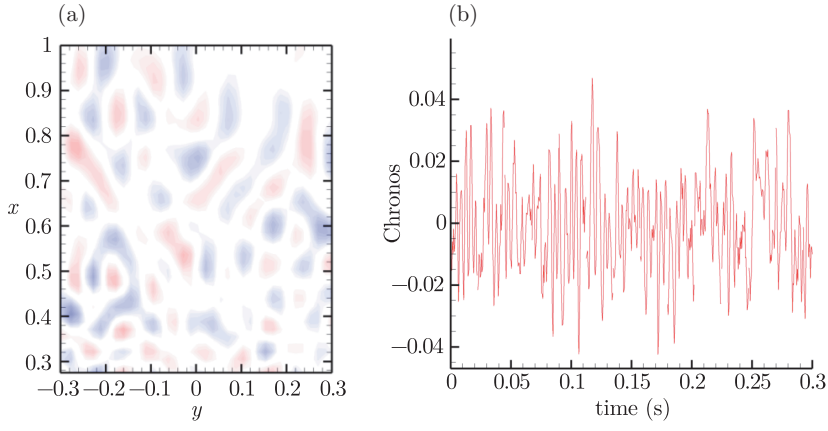

Figure 15. Topos (a) and Chronos (b) of the POD mode 99

fill the studied region regularly with smaller and more randomly distributed structures. The Chronoses of the higher order POD modes show an increasing content of higher frequencies – compare Chronos 1 (Figure 12 (b)) with Chronos 99 (Figure 15 (b)). All Chronoses are random in nature.

5. Conclusions

The topology of the flow in the vicinity of the suction surface of the flat plate in the regular stream with the angle of attack 7° was studied experimentally. The time resolved PIV method was applied with the measuring plane located close to the plate surface and parallel thereto.

Both the velocity and the vorticity fields were explored in details. While the time-mean flow-field was close to 2D structure, the dynamical structures were mostly 3D. The typical structures topology in the form of streamwise streaks and

zigzag patterns is shown. The flow-structures form waves travel in the streamwise direction.

Acknowledgements

This work was supported by the Grant Agency of the Czech Republic, Project No. 17–01088S.

References

[1] Uruba V, Pavlík D, Procházka P, Skála V and Kopecký V 2017 *EPJ Web of Conferences* **143** 2137
[2] Uruba V, Pátek Z, Procházka P, Skála V, Zacho D and Kulhánek R 2018 *EPJ Web of Conferences* **180** 2111
[3] Uruba V, Procházka P and Skála V 2018 *EPJ Web of Conferences* **180** 2112
[4] Procházka P, Uruba V and Skála V 2018 *Journal of Physics Conference Series* **1101** UNSP 12026
[5] Hoffman J and Johnsson C 2009 *Normat* **57** (4) 1
[6] Lumley J L 1967 *Atm. Turb. and Radio Wave Prop.* 166, Yaglom and Tatarsky eds., Nauka, Moskva
[7] Hasselmann K 1988 *Journal of Geophysical Research* **93** (D9) 11
[8] Uruba V 2012 *EPJ Web of Conferences* **25** 1095
[9] Uruba V 2015 *Journal of Fluids and Structures* **55** 372